NUMERICAL SIMULATION OF BLAST PRESSURE ON ACCESS BLAST DOOR USING ABAQUS SOFTWARE

Duc Thao Pham[1,*], Ngoc Thuy Ngo[1], Van Loi Tran[2]

[1]*Institute of Techniques for Special Engineering, Le Quy Don Technical University*

[2]*Ngo Quyen Technical University*

Abstract

This article presents the investigation results of reflected blast pressure acting on access blast doors using a numerical simulation method with Abaqus software. The study employs Sadovskii's empirical formula as the theoretical basis for determining shock wave overpressure. Simulations were conducted with parametric variations including: TNT explosive mass ranging from 50 kg to 200 kg, standoff distance from explosion center to protective door (R_0) from 10m to 25m, and incident angle α between shock wave propagation direction and door surface normal from 0° to 60°, under the assumption that the protective door is perfectly rigid and immobile. Results show that the error between Abaqus simulation and empirical formula ranges from 1.123% to 13.65%, demonstrating high reliability of the simulation method. Reflected pressure decreases with increasing standoff distance R_0 and varies complexly with angle α due to the curved surface characteristics of the protective door. The study confirms that Abaqus software is an effective tool for predicting and analyzing blast pressure on protective door structures, contributing to improved efficiency and safety in the design and construction of access tunnel protective doors in practice. Moreover, the influence of the curvature radius of the door surface on the reflected pressure value is complex. When calculating the load acting on the protective door, it is necessary to consider the average reflected pressure on the curved surface to ensure accurate calculations.

Keywords: *Shock wave; reflected pressure; protective door; numerical simulation; Abaqus; surface burst; blast loading; tunnel structure.*

1. Introduction

In the context of modern conflicts, the use of precision-guided flying objects has increased the risk of destruction to defensive structures, particularly tunnel entrances and protective structures, which are subjected to direct impact from blast loads. Therefore, research on the behavior of shock waves and their interaction with protective structures, including protective doors, is an urgent issue in order to propose reinforcement solutions and enhance defense effectiveness.

Globally, research on the response of protective doors under blast loading has been widely conducted. Chen *et al.* [1] performed rate-sensitive numerical analysis of

[*] Corresponding author, email: ryodan1997@gmail.com
DOI: 10.56651/lqdtu.jst.v8.n2.1086.sce

the dynamic response of arched blast doors subjected to blast loading. Li *et al.* [2] investigated factors influencing the anti-explosion performance of steel structure protective doors under chemical explosion conditions using numerical simulation methods. Pranata and Madutujuh [3] used dynamic time history analysis to evaluate blast-resistant doors when modeling blast loads as impact loads. Veeredhi and R. Rao [4] studied the impact of explosions on stiffened blast-resistant door structures. Al-Rifaie and Sumelka [5] improved the blast resistance of large steel gates through numerical studies, while Li *et al*. [6] investigated the blast performance of multi-layer composite door panels with energy absorption connectors. Schneider and Großmann [7] reviewed design methods for blast-resistant façades, windows, and doors in Germany. Abaqus with the CONWEP model has demonstrated high efficiency in simulating shock waves and their effects on structures with very small errors [8], [9]. This method allows observation of the formation and effects of blast waves on structures, predicting results thereby helping to conduct field experiments more efficiently and safely.

In Vietnam, research on blast loads has begun to receive attention in recent years. L. B. Danh [10] investigated numerical models for simulating blast loads on reinforced concrete structures using Abaqus, comparing three methods: SPH, equivalent blast charge, and CEL. P. T. Trung [11], [12] focused on simulating protection solutions for reinforced concrete structures and evaluating the failure of reinforced concrete columns under contact blast loads through both numerical simulation and field experiments.

L. B. Danh *et al.* [13] and D. H. Pham *et al*. [14] conducted experimental studies on the blast load resistance of UHPC and conventional concrete. N. X. Bang *et al*. [15] investigated local failure of fiber-reinforced concrete slabs under blast loading using LS-DYNA. N. Q. Tuan *et al*. [16] analyzed the effects of explosions on arched steel bridge structures.

Research on the propagation characteristics and interaction of shock waves has also received attention. N. N. Thuy [17] used Ansys Autodyn 3D to determine shock wave pressure values for simultaneous multiple explosions acting on structure roofs. D. T. Thang *et al*. [18] studied the attenuation of blast stress waves propagating in limestone environments. N. X. Bang [19] investigated shock wave pressure under various explosion scenarios using simulation methods.

Although there has been considerable research on blast loads acting on reinforced concrete structures and blast doors, studies in Vietnam remain limited. Therefore, this research aims to investigate reflected blast pressure values acting on access blast doors using numerical simulation methods with Abaqus software. The study focuses on analyzing the influence of explosive mass (50-250 kg TNT), standoff distance (10-25 m),

and particularly the incident angle α between the shock wave propagation direction and door surface normal (0°-60°) on reflected pressure values. The research results will provide a scientific basis for the design and load-bearing capacity evaluation of access tunnel protective doors, while helping to optimize future field experiments.

2. Theoretical background

2.1. Blast wave fundamentals

- When an explosive detonates, the rapid release of chemical energy generates an extremely high-pressure shock front that propagates through the surrounding medium at supersonic velocity. This shock wave, commonly referred to as a blast wave, consists of two distinct phases: the positive pressure phase and the negative pressure (suction) phase. The positive phase is characterized by an instantaneous rise in pressure to a peak overpressure value (ΔP_{max}), followed by an exponential decay back to ambient pressure over a duration t^+. The negative phase, which follows immediately, has a longer duration but typically lower magnitude compared to the positive phase.

- The blast wave parameters of primary concern for structural analysis include:

+ Peak overpressure (ΔP_{max}): The maximum pressure above atmospheric pressure;

+ Impulse (I): The integral of pressure over time, representing the total energy delivered;

+ Positive phase duration (t^+): The time period during which overpressure exists;

+ Arrival time (t_a): The time for the shock front to reach a specified location.

- These parameters are functions of the explosive yield, standoff distance, and environmental conditions. For surface bursts, where the explosive is detonated on or near the ground surface, the blast wave propagates hemispherically rather than spherically. This geometric constraint effectively concentrates the explosive energy into half the volume, resulting in significantly higher overpressures compared to free-air bursts at equivalent standoff distances.

2.2. Sadovskii's empirical formula

Sadovskii developed empirical relationships through extensive field experiments to predict shock wave overpressure in air [20]. For explosions in infinite air space (free-air burst), the peak overpressure at distance R from the explosion center is given by:

$$\Delta P_{\Phi} = 84\frac{\sqrt[3]{C}}{R} + 270\left(\frac{\sqrt[3]{C}}{R}\right)^2 + 700\left(\frac{\sqrt[3]{C}}{R}\right)^3 \quad \text{(kPa)} \tag{1}$$

where ΔP_{Φ} is the peak overpressure (kPa), C is the total equivalent TNT mass (kg), R is the standoff distance from explosion center (m).

For surface bursts, nearly all the explosion energy is concentrated into a hemispherical blast wave. Consequently, the overpressure can be approximated by considering an equivalent charge mass of 2*C* in Eq. (1):

$$\Delta P_{\Phi} = 106\frac{\sqrt[3]{C}}{R} + 430\left(\frac{\sqrt[3]{C}}{R}\right)^2 + 1400\left(\frac{\sqrt[3]{C}}{R}\right)^3 \quad \text{(kPa)} \tag{2}$$

When a shock wave propagating along the ground encounters a rigid, stationary surface structure, a reflection process occurs. The reflected pressure acting on the immovable obstacle is determined by the following formula:

$$\Delta P_{fx} = 2\Delta P_{\Phi} + \frac{6\Delta P_{\Phi}^2}{\Delta P_{\Phi} + 720} \quad \text{(kPa)} \tag{3}$$

where ΔP_{fx} is the reflected shock wave pressure (kPa).

The positive phase duration for the shock wave compression phase is estimated by [21]:

$$\frac{a_1}{r_0}\tau_+ = \begin{cases} 9 & \text{when } \dfrac{r}{r_0} < 28 \\ 1.8\sqrt{\dfrac{r}{r_0}} & \text{when } 28 < \dfrac{r}{r_0} < 150 \\ 4.2\sqrt[3]{\dfrac{r}{r_0}} & \text{when } \dfrac{r}{r_0} > 150 \end{cases} \tag{4}$$

where a_1 is the speed of sound in the undisturbed medium (m/s), r is the standoff distance from explosion center (m), r_0 is the radius of the explosive charge (m).

2.3. CONWEP model

2.3.1. Overview and development

These empirical formulas have been widely validated and form the basis for many blast design codes and standards. However, they are applicable only to idealized conditions including homogeneous atmosphere, flat terrain, and sufficient standoff distance to avoid near-field effects.

The fundamental principle underlying CONWEP is the concept of scaled distance, defined as:

$$Z = \frac{R}{W^{1/3}} \tag{5}$$

where Z is the scaled distance ($\mathrm{m/kg^{1/3}}$), R is the standoff distance (m), W is the TNT equivalent charge mass (kg).

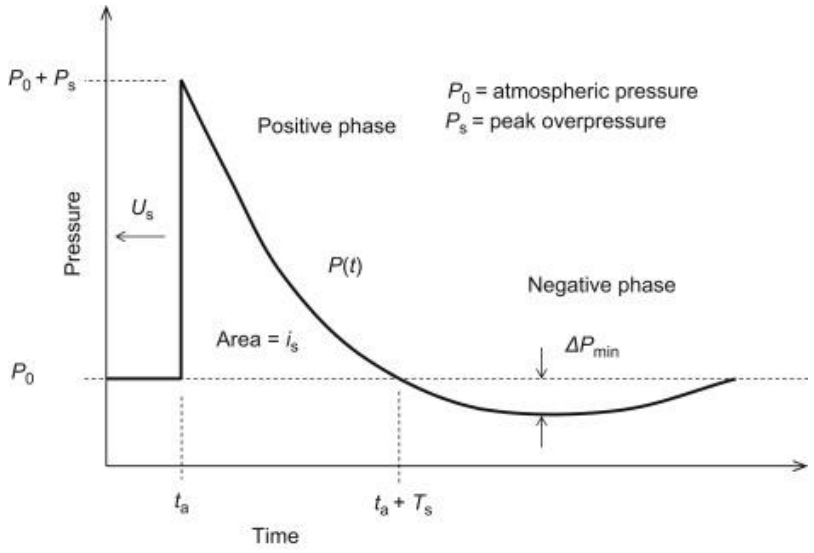

Fig. 1. Graph of shock wave pressure values.

This scaling law, known as Hopkinson-Cranz scaling or cube-root scaling, allows blast parameters from one charge mass to be extrapolated to different charge masses, provided geometric and atmospheric conditions remain similar.

2.3.2. Implementation in Abaqus

Abaqus/Explicit incorporates the CONWEP library to enable efficient blast load simulation without requiring detailed modeling of the explosive, detonation products, and air domain. When the CONWEP load option is invoked, Abaqus automatically calculates the incident blast pressure $P(t)$ at each node or integration point on the specified surface based on:

+ The standoff distance R from the explosion center to the point;

+ The TNT equivalent charge mass W;

+ The angle of incidence α between the shock wave propagation direction and the surface normal [22].

- The software interpolates from internal CONWEP tables to determine: Peak incident overpressure (P_{SO}); Peak reflected overpressure (P_r); Positive phase duration (t^+); Impulse (I); Wave arrival time (t_a). Wave decay coefficient.

The time-dependent pressure history $P(t)$ is then applied as a distributed load on the structure surface. For reflected pressure on a rigid surface, the modified Friedlander equation is used:

$$P(t) = P_r\left(1 - \frac{t - t_a}{t^+}\right)e^{-b(t-t_a)/t^+} \quad \text{for } t_a \le t \le t_a + t^+ \tag{6}$$

where P_r is the peak reflected pressure, t_a is the arrival time, t^+ is the positive phase duration, *b* is the decay coefficient (typically 1-2).

2.4. Reflected pressure on surfaces

2.4.1. Normal reflection

When a blast wave encounters a rigid obstacle perpendicular to its propagation direction (normal incidence, α = 0°), the shock wave reflects, creating a reflected overpressure P_r that significantly exceeds the incident overpressure P_{SO}. The reflection amplification factor depends on the shock wave strength and can be estimated from Rankine-Hugoniot relations for strong shocks:

$$\frac{P_r}{P_{SO}} = \frac{2\left(7P_0 + 4P_{SO}\right)}{7P_0 + P_{SO}} \tag{7}$$

where P_0 is the ambient atmospheric pressure (typically 101.325 kPa). For moderate to strong blast waves (P_{SO} > 70 kPa), the reflected pressure can be 2 to 8 times the incident pressure. This amplification is the primary reason structures subjected to blast loading experience much higher loads than predicted by incident pressure alone.

2.4.2. Oblique reflection

- For oblique incidence (α > 0°), the reflected pressure decreases as the incident angle increases. The relationship is nonlinear and depends on: Incident angle α; shock wave strength (Mach number); surface geometry (flat, curved, irregular).

- For flat surfaces at oblique angles, empirical relationships have been developed [2]. However, for curved surfaces such as the protective door investigated in this study, the reflection phenomenon is more complex due to:

+ Varying local incident angles across the surface;

+ Wave focusing or defocusing effects depending on curvature;

+ Multiple reflection interactions;

+ Shadow zones behind curved features.

2.4.3. Curved surface effects

The curved geometry of the protective door introduces additional complexity to the reflected pressure distribution. As the blast wave propagates, different portions of the curved surface experience different incident angles simultaneously. At the center of the door (assuming the explosion is directly in front), the incident angle approaches 0°, yielding maximum reflected pressure. Moving toward the edges, the incident angle increases, resulting in lower reflected pressures.

Curvature can induce wave-focusing effects, leading to localized pressure amplification, whereas certain geometries may defocus the blast wave, thereby reducing the overall load. These three-dimensional effects cannot be reliably predicted by one-dimensional empirical formulas and require numerical simulation for accurate characterization.

2.5. Research assumptions and simplifications

To enable tractable numerical analysis while maintaining reasonable accuracy, this study adopts several simplifying assumptions. These assumptions are categorized into structural, blast loading, and modeling considerations, each justified by their minimal impact on the primary research objectives while significantly reducing computational complexity.

2.5.1. Structural assumptions

The following assumptions are made regarding the protective door structure:

- Rigid body assumption: The protective door is modeled as a rigid, non-deformable body under blast loading. This conservative approach ensures that the calculated blast pressures represent the upper bound of loading conditions. By decoupling structural deformation from blast wave propagation, this assumption simplifies the analysis while maintaining a safety margin in pressure predictions. For preliminary design studies focusing on blast load characterization rather than structural response, this assumption is widely accepted.

- Fixed boundary conditions: The door is assumed to be perfectly restrained at all boundary edges, representing ideal anchorage without slip or rotation. This represents the best-case scenario for load transfer to the surrounding structure and is consistent with well-designed protective door installations.

2.5.2. Blast loading assumptions

The blast loading conditions are defined by the following assumptions:

- Surface burst configuration: All explosions are modeled as hemispherical surface bursts with the explosive charge center positioned at ground level. This configuration represents the most severe and commonly considered threat scenario for protective structures, as it concentrates blast energy into the hemisphere above ground [3].

- TNT equivalency: All explosive materials are expressed in TNT equivalent mass, enabling direct application of CONWEP empirical data. This standardization is essential for consistent analysis and is achieved through established conversion factors available in the literature for various explosive types.

- Standard atmospheric conditions: The analysis assumes standard atmospheric pressure (101.325 kPa), temperature (15°C), and relative humidity (50%). Environmental effects such as wind, atmospheric turbulence, temperature gradients, and altitude variations are neglected. These simplifications are reasonable for controlled parametric studies and are consistent with CONWEP database conditions.

2.5.3. Modeling assumptions

The numerical model incorporates the following assumptions:

- Hemispherical wave propagation: The blast wave is assumed to propagate uniformly as a hemispherical front expanding from the detonation point. This idealization is valid for surface bursts on flat, unobstructed terrain and is consistent with the theoretical basis of the CONWEP model.

- Pressure loading only: The analysis focuses exclusively on blast overpressure effects. Secondary effects including fragment impact, crater ejecta, ground shock transmission, and thermal radiation are not considered. For protective door design at the standoff distances studied (10-25) m, overpressure is typically the dominant loading mechanism.

- Decoupled analysis approach: The blast pressure calculation and structural response analysis are treated as separate, sequential processes. This is justified when the structural response time scale (natural period of the door) is significantly longer than the blast loading duration, preventing significant feedback from structural motion to the incident blast wave.

2.5.4. Validity range and applicability

- The above assumptions are valid within the following parameter ranges:

+ Scaled distance: $Z > 0.4\ \mathrm{m/kg^{1/3}}$, ensuring far-field blast regime where CONWEP empirical relationships are most accurate;

+ Peak overpressure: $\Delta P < 2$ MPa, remaining within the validated range of CONWEP database;

+ Standoff distance: $R > 5$ m, avoiding near-field complexities such as cratering, ground shock coupling, and close-in effects.

- These parametric bounds encompass typical threat scenarios for protective structures while maintaining the validity of the employed theoretical and numerical methods.

2.5.5. Implications and limitations

- The adopted simplifications enable efficient parametric analysis suitable for:

Preliminary design optimization; Comparative studies of geometric configurations; Sensitivity analysis of key parameters; Rapid evaluation of multiple threat scenarios.

- However, these assumptions introduce limitations that should be recognized:

+ Rigid body assumption yields conservative (higher) pressure predictions but cannot capture load mitigation through structural flexibility;

+ Neglecting fragment impact may underestimate total loading in certain scenarios;

+ Standard atmospheric conditions may not represent all operational environments.

For final design validation and high-consequence applications, more sophisticated analyses incorporating coupled fluid-structure interaction (FSI), material nonlinearity, and fragment effects should be considered.

3. Simulation

This study investigated the impact of surface explosions 10 to 25 meters from the tunnel entrance, focusing on the shock wave pressure acting on the outer surface of the protective door. Charge mass: from 50 kg to 250 kg TNT, the survey point is located on the outer surface of the protective door (point A model coordinate 198; point B model coordinate 90; point C model coordinate 18; point B' coordinate model 270; point C' coordinate model 344), the dimensions of the protective door are as follows: B = 0.9 (m); H = 1.8 (m) (Fig. 2). The location of the protective door is at the starting point of the tunnel (Fig. 3).

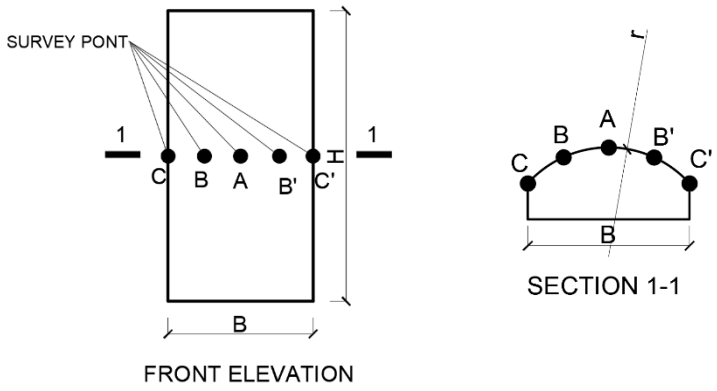

Fig. 2. Model of protective door and survey points.

To investigate the effect of shock waves on the protective door, this study employs the CONWEP/Abaqus explosion model with charge mass varying from 50 kg to 250 kg and the standoff distance from the detonation point to the protective door (R) varying from 10 meters to 25 meters.

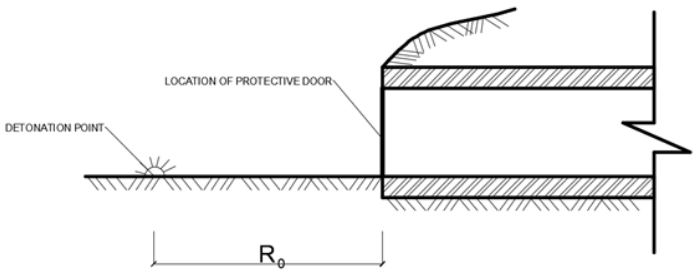

Fig. 3. Plan of protective door.

* The standoff distance varying from 10 (m) to 25 (m) with charge mass = 50 kg.

The reflected overpressure at the midpoint of the door (Point A) at a standoff distance of 25 (m) is presented in Fig. 4. In Fig. 5, the distribution of the reflected overpressure acting on the door from a standoff distance of 25 (m) can be observed. The simulation results are summarized in Tab. 1. In Tab. 1, this study compares the simulation results with the results calculated using empirical formula (7).

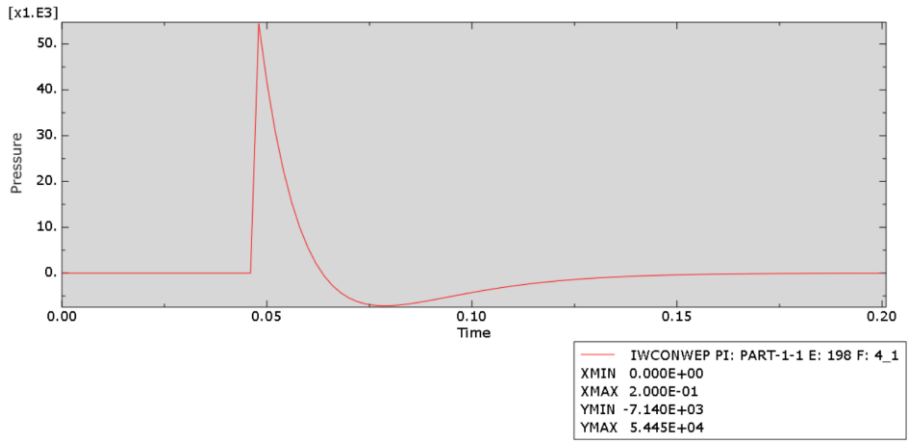

Fig. 4. The reflected overpressure value at point A at a standoff distance of R = 25 m.

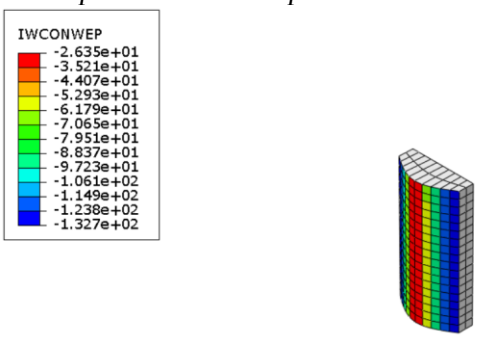

Fig. 5. The reflected overpressure value on protective door's surface at a standoff distance of R = 25 m.

Tab. 1. Table comparing the reflected overpressure values for charge mass of 50 kg, with the standoff distance R varying from 10 m to 25 m

No.	Standoff distance (m)		Reflected overpressure value		
			Empirical formulas (kPa)	Abaqus (kPa)	Error (%)
1	10	Point A	**434.16**	416.9	3.975
		Point B		362.09	
		Point C		305.9	
		Point B’		362.1	
		Point C’		324.5	
2	15	Point A	**155.79**	150.7	3.267
		Point B		132.1	
		Point C		127.98	
		Point B’		135.25	
		Point C’		127.22	
3	20	Point A	**85.78**	84.77	1.177
		Point B		68.6	
		Point C		68.03	
		Point B’		74.31	
		Point C’		68.12	
4	25	Point A	**57.59**	54.45	5.452
		Point B		51.67	
		Point C		39.63	
		Point B’		51.73	
		Point C’		39.66	

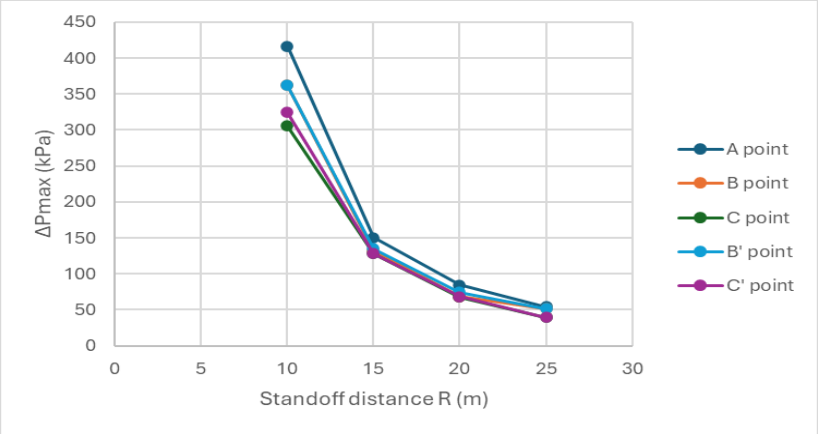

Fig. 6. Graph of pressure values as a function of standoff distance R.

From these simulation results, the graph of pressure values curve corresponding to the variation of the standoff distance R is obtained, as shown in Fig. 6.

* The charge mass (C) varying from 50 kg to 200 kg with standoff distance R = 25 m:

The reflected overpressure at the midpoint of the door (Point A) for a charge mass of 100 kg is presented in Fig. 7. Along with this, Tab. 2 presents the summarized simulation results for charge mass ranging from 50 kg to 200 kg, and Fig. 8 shows the corresponding consolidated pressure-charge diagram.

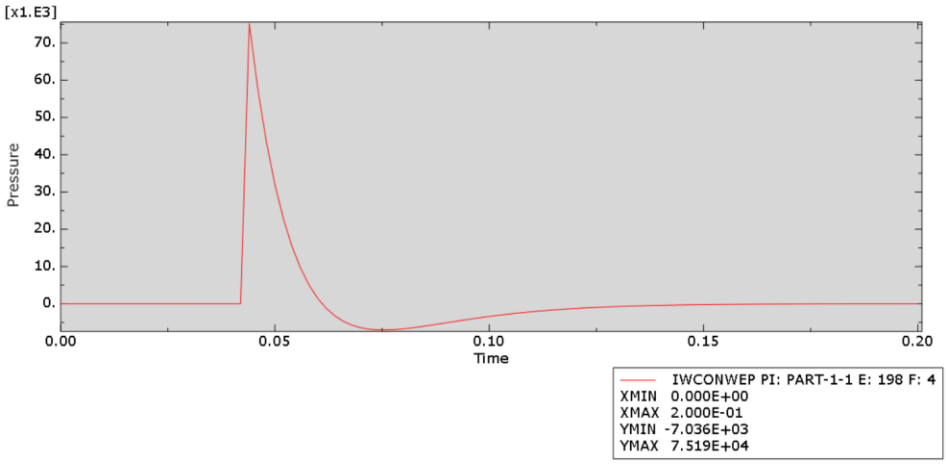

Fig. 7. The reflected overpressure value at point A with charge mass C = 100 kg.

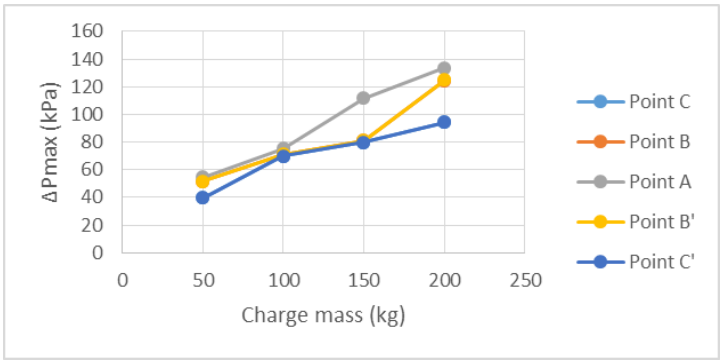

Fig. 8. Graph of pressure values as a function of charge mass C.

From the simulation results, it can be observed that the reflected pressure values at different points on the curved surface of the door vary. This indicates that the radius r of curvature of the door surface affects the reflected pressure acting on the door, and this parameter should be further investigated when determining the load applied to the door.

To investigate the influence of the door surface curvature radius on the reflected pressure acting on the door, this study employs the CONWEP/Abaqus explosion model

with charge (*C*) equal 50 kg and the standoff distance from the detonation point to the protective door (*R*) equal 25 meters and the radius of curvature of the door surface (*r*) varying from 0.45 meters to 0.9 meters. When varying the radius of curvature, the position of the protective door was adjusted to ensure that the minimum distance from the curved door surface to the explosive charge location remained constant at 25 (m).

Tab. 2. Comparing the reflected overpressure values for charge mass varying from 50 kg to 200 kg, with the standoff distance R_0 = 25 m

No.	Charge mass (kg TNT)		Reflected overpressure value		
			Empirical formulas (kPa)	Abaqus (kPa)	Empirical formulas (kPa)
1	50	Point A	**57.59**	54.45	5.452
		Point B		51.68	
		Point C		39.63	
		Point B’		51.73	
		Point C’		39.66	
2	100	Point A	**87.08**	75.19	13.65
		Point B		71.00	
		Point C		69.97	
		Point B’		71.09	
		Point C’		70.02	
3	150	Point A	**113.92**	111.8	1.861
		Point B		81.09	
		Point C		79.91	
		Point B’		81.19	
		Point C’		79.97	
4	200	Point A	**139.77**	133.65	4.379
		Point B		124.65	
		Point C		94.18	
		Point B’		124.83	
		Point C’		94.26	

The reflected overpressure at the midpoint of the door (Point A) for a door curvature radius of r = 0.90 (m) is presented in Fig. 9 and Tab. 3 summarizes the simulation results for the cases with varying door curvature radii. It can be observed that the reflected pressure values acting on points A, B, and B' increase as the curvature radius of the door surface increases, while the pressure at point C and C' decreases when the curvature radius increases from 0.45 (m) to 0.75 (m), then increases again as the curvature radius increases from 0.75 (m) to 0.90 (m) (Fig. 10).

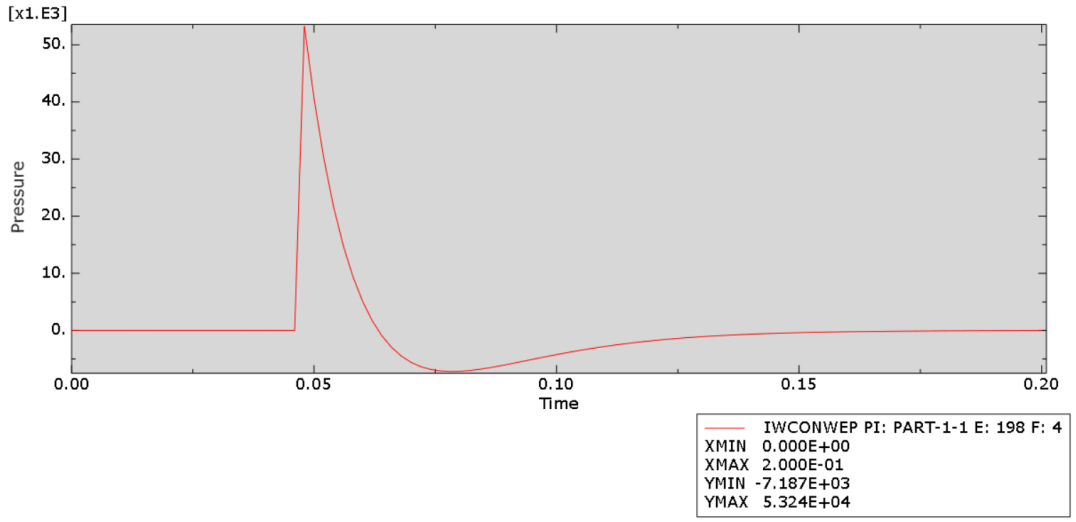

Fig. 9. The reflected overpressure value at point A with radius of curvature of the door surface r = 0.90 (m).

Tab. 3. Table comparing the reflected overpressure values for radius of curvature of the door surface varying from 0.45 m to 0.90 m, with the charge mass C = 50 kg and the standoff distance R_0 = 25 m

No.	Survey point	Reflected overpressure value (kPa)			
		r = 0.45 m	*r* = 0.60 m	*r* = 0.75 m	*r* = 0.90 m
1	A	44.91	54.449	53.69	53.24
2	B	42.89	51.676	50.97	50.57
3	C	42.61	39.627	39.05	50.04
4	B’	42.93	51.728	51.04	50.62
5	C’	42.65	39.663	39.08	50.08

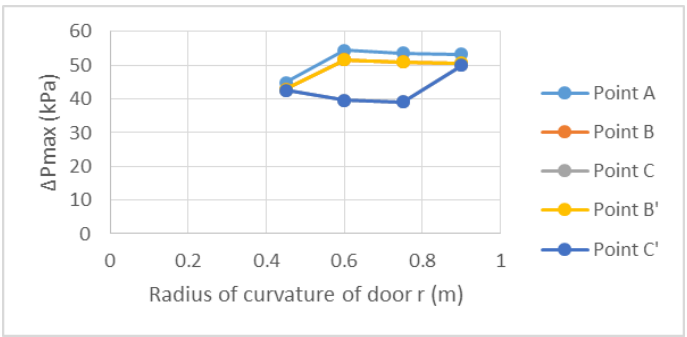

Fig. 10. Graph of pressure values as a function of radius of curvature of the door surface r.

In cases where the charge mass and the curvature radius of the door surface are varied, certain nonlinear variations in the reflected blast pressure can be observed at points B, B′, C, and C′. This phenomenon occurs because the peak reflected pressure depends on the scaled stand-off distance and the reflection angle between the incident

shock wave and the structural surface. This angle typically ranges from 45° to 80°, depending on the intensity of the incident shock wave [23].

Given the curved surface of the blast door, this study investigates the reflected overpressure by varying the incident angle (α) between the shock wave propagation direction and the door normal. The analysis considers three aligned points: the center (D02, model coordinate 198) and two edge points (D01 and D03, model coordinates 18 and 344), for a charge mass of 50 kg TNT equivalent and a standoff distance of 25 (m) (Fig. 11).

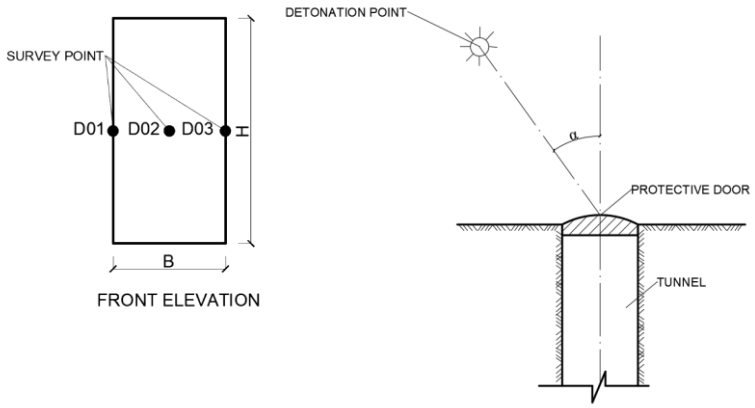

Fig. 11. Diagram of survey points on the protective door for the case of varying the shock wave propagation direction relative to the protective door's normal.

As the inclination angle α between the wave propagation direction and the normal of the protective door surface increases from 0° to 60°, the pressure values at points D01 and D02 respectively gradually decrease from 50.158 kPa to 24.92 kPa and from 57.02 kPa to 43.11 kPa (Tab. 4). The graph of the pressure values at point D02 with a 50 kg charge mass at a stand off distance of 25 m, where the shock wave propagation direction forms an angle of α = 30° with the normal of the protective door is presented in Fig. 12.

Tab. 4. Table comparing the reflected overpressure values when the shock wave propagation direction forms an angle from 0° to 60° with the normal of the protective door, for a charge mass of C = 50 kg and a standoff distance of R_0 = 25 m

No.	**Survey point**	**Reflected overpressure value (kPa)**			
		0°	30°	45°	60°
1	D01	50.158	37.06	30.07	24.92
2	D02	57.02	54.12	49.38	43.11
3	D03	49.89	57.48	56.95	54.26

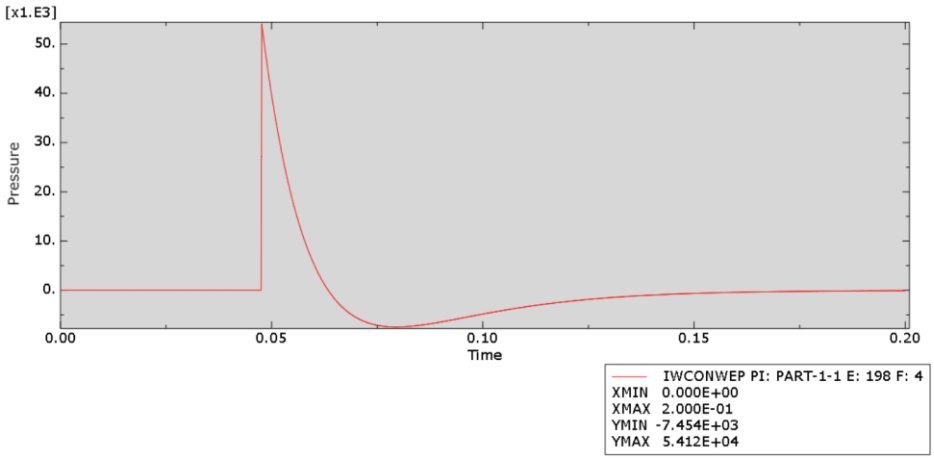

Fig. 12. Reflected overpressure value at point D02 with a 50 kg charge mass at a standoff distance of 25 (m), where the shock wave propagation direction forms an angle of α = 30° with the normal of the protective door.

At point D03, the pressure increases from 48.89 kPa to 57.48 kPa and then decreases to 54.26 kPa (Fig. 13). This phenomenon occurs because the surface of the protective door is curved, when an offset angle α appears between the wave propagation direction and the protective door's normal toward point D03, the distance from D03 to the explosion center becomes greater compared to points D01 and D02.

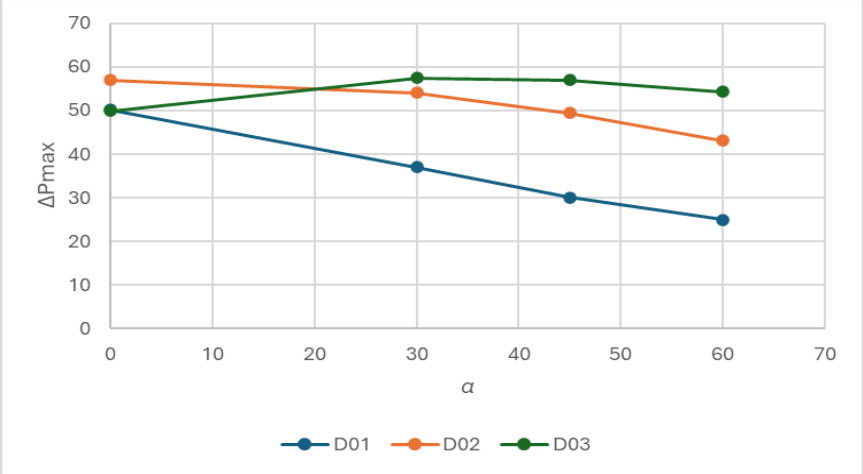

Fig. 13. Graph of pressure values versus angle α between the wave propagation direction and the normal of the protective door.

4. Conclusion

With these results we can observe that the simulation results differ from 1.123% to 13.65% compared with the empirical formula results in cases of varying explosive charge weight and standoff distance to the surveyed surface. These results indicate that the

CONWEP simulation model can be reliably employed to study reflected shock waves on material surfaces under blast loading, allowing the observation of variations in blast pressure on structural surfaces, as well as the prediction of outcomes to enhance efficiency and safety in conducting real experiments. Moreover, the influence of the curvature radius of the door surface on the reflected pressure is complex and is not fully captured by existing empirical formulas. When calculating the loads acting on the protective door, it is necessary to consider the average reflected pressure over the curved surface obtained from numerical simulation models in order to ensure accurate results.

Acknowledgement

This research is funded by Le Quy Don Technical University Research Fund under the grant number 25.10.53

References

[1] L. Chen, Q. Fang, Y. Zhang, and Y. Zhang, "Rate-sensitive numerical analysis of dynamic responses of arched blast doors subjected to blast loading", *Transactions of Tianjin University*, Vol. 14, Iss. 6, pp. 435-440, 2008. DOI: 10.1007/s12209-008-0059-x

[2] J. Li, J. Wang, X. Chen, and Y. Zhao, "Numerical simulation study on factors influencing anti-explosion performance of steel structure protective doors under chemical explosion conditions", *International Journal of Protective Structures*, Vol. 13, No. 2, pp. 123-138, 2022. https://pubmed.ncbi.nlm.nih.gov/35683179/

[3] Y. A. Pranata and N. Madutujuh, "Dynamic time history analysis of blast resistant door using blast load modeled as impact load", *Journal of the Civil Engineering Forum*, Vol. 1, No. 1, pp. 47-54, 2012. https://journal.ugm.ac.id/jcef/article/view/18934

[4] L. S. B. Veeredhi and N. V. R. Rao, "Studies on the impact of explosion on blast resistant stiffened door structures", *Journal of The Institution of Engineers (India): Series A*, Vol. 96, pp. 43-52, 2015. DOI: 10.1007/s40030-014-0103-x

[5] A. Al-Rifaie and W. Sumelka, "Improving the blast resistance of large steel gates - Numerical study", *Materials*, Vol. 13, Iss. 9, pp. 1-21, 2020. DOI: 10.3390/ma13092121

[6] Z. Li, W. Liu, C. Zhang, and J. Wang, "Blast performance of multi-layer composite door panel with energy absorption connectors", *Buildings*, Vol. 15, Iss. 12, 2025. DOI: 10.3390/buildings15122073

[7] J. Schneider and F. Großmann, "Design methods of blast resistant façades, windows, and doors in Germany: A review", *Glass Structures & Engineering*, Vol. 7, No. 2, pp. 145-166, 2022. DOI: 10.1007/s40940-022-00213-w

[8] Dassault Systèmes, *ABAQUS Analysis User's Guide: Explicit dynamics and blast loading*. Providence, RI: Dassault Systèmes Simulia Corp., 2014.

[9] Dassault Systèmes. *ABAQUS Documentation: Coupled Eulerian–Lagrangian (CEL) analysis for blast and penetration problems*. Providence, RI: Dassault Systèmes Simulia Corp., 2017.

[10] L. B. Danh, "Nghiên cứu các mô hình số mô phỏng tải trọng nổ lên kết cấu bê tông cốt thép sử dụng phần mềm Abaqus", *Tạp chí Khoa học Giao thông Vận tải*, Tập 74, Số 2, tr. 139-149, 2023.

[11] P. T. Trung, "Mô phỏng giải pháp bảo vệ kết cấu bê tông cốt thép dưới tác dụng của tải trọng nổ tiếp xúc", *Tạp chí Khoa học Công nghệ Xây dựng – Viện KHCN Xây dựng*, Số 3/2023, tr. 20-26, 2023. DOI: 10.59382/j-ibst.2023.vi.vol3-3

[12] P. T. Trung, N. Q. Bảo và V. Đ. Hiếu, "Đánh giá sự phá hủy cấu kiện cột bê tông cốt thép dưới tác dụng tải trọng nổ tiếp xúc bằng mô phỏng số và thực nghiệm tại hiện trường", *Tạp chí Khoa học Công nghệ Xây dựng – Trường Đại học Xây dựng Hà Nội*, Tập 14, Số 5V, tr. 180-196, 2020. DOI: 10.31814/stce.nuce2020-14(5V)-15

[13] L. B. Danh và nnk, "Nghiên cứu thực nghiệm khả năng chịu tác động tải trọng nổ của vật liệu bê tông chất lượng siêu cao (UHPC)", *Tạp chí Khoa học Công nghệ Xây dựng*, Tập 13, Số 3V, tr. 12-21, 2019. DOI: 10.31814/stce.nuce2019-13(3V)-02

[14] D. H. Pham *et al*., "A comparison between experimental and numerical studies of RC slabs under explosive loading", *Geomate Journal*, Vol. 22, Iss. 93, pp. 1-8, 2022. DOI: 10.21660/2022.93.j2378

[15] N. X. Bàng, "Nghiên cứu sự phá hoại cục bộ của tấm bê tông cốt sợi dưới tải nổ", *Tạp chí Khoa học Công nghệ Xây dựng – Trường Đại học Xây dựng Hà Nội*, Tập 17, Số 4V, tr. 100-113, 2023. DOI: 10.31814/stce.huce2023-17(4V)-09

[16] N. Q. Tuấn, "Nghiên cứu ảnh hưởng của tác dụng nổ lên kết cấu cầu thép dạng vòm", *Tạp chí Xây dựng*, Số 06/2025, tr. 304-309, 2025.

[17] N. N. Thủy, "Xác định giá trị áp lực sóng nổ của các vụ nổ đồng thời tác dụng lên nóc công trình", *Tạp chí Khoa học Công nghệ Xây dựng*, Số 1-2021, tr. 33-39, 2021.

[18] Đ. T. Thắng, N. N. Thủy và N. T. Đức, "Nghiên cứu sự suy giảm sóng ứng suất nổ khi lan truyền trong môi trường đá vôi", *Tạp chí Xây dựng*, Số 11/2023, tr. 70-75, 2023.

[19] N. X. Bàng, "Nghiên cứu áp lực sóng xung kích khi xảy ra nổ đồng thời", *Tạp chí Khoa học Công nghệ Xây dựng*, Tập 17, Số 4V, tr. 168-178, 2023. DOI: 10.31814/stce.huce2023-17(4V)-14

[20] M. A. Sadovskii, "The mechanical effect of blastwaves in air with respect to data from experimental studies", in *Physics of Explosions*, Collection No. 1, AN SSSR, Moscow, 1952, pp. 20-111.

[21] H. S. Giao và nnk, *Nổ hóa học lý thuyết & thực tiễn*, Nxb Khoa học và Kỹ thuật, 2010.

[22] *Microcomputer Programs CONWEP and FUNPRO: Applications of TM 5-855-1*. U.S. Army Engineer Waterways Experiment Station, ADA195867, 1988.

[23] UFC 3-340-02, U.S. Army Corps of Engineers supersedes ARMY TM 5-1300, NAVFAC P-397 and AFR 88-22 dated November 1990.

MÔ PHỎNG ÁP LỰC NỔ TÁC DỤNG LÊN CỬA CÔNG TRÌNH BẰNG PHẦN MỀM ABAQUS

Phạm Đức Thảo[1], Ngô Ngọc Thủy[1], Trần Văn Lợi[2]

[1]*Viện Kỹ thuật công trình đặc biệt, Trường Đại học Kỹ thuật Lê Quý Đôn*

[2]*Trường Đại học Ngô Quyền*

Tóm tắt: Bài báo trình bày kết quả nghiên cứu về áp lực sóng phản xạ tác dụng lên cửa công trình bằng phương pháp mô phỏng sử dụng phần mềm Abaqus. Nghiên cứu sử dụng công thức thực nghiệm của Sadovskii làm cơ sở lý thuyết để xác định giá trị áp lực sóng xung kích. Các mô phỏng được thực hiện với các tham số thay đổi gồm: khối lượng thuốc nổ TNT từ 50 kg đến 200 kg, khoảng cách từ tâm nổ đến cửa công trình (R_0) từ 10 m đến 25 m, và góc tới α giữa phương truyền sóng xung kích và pháp tuyến bề mặt cửa từ 0° đến 60° với điều kiện cửa công trình là tuyệt đối cứng, bất động. Kết quả cho thấy sai số giữa mô phỏng Abaqus và công thức thực nghiệm nằm trong khoảng từ 1,123% đến 13,65%, chứng tỏ độ tin cậy cao của phương pháp mô phỏng. Áp lực phản xạ giảm dần khi khoảng cách R_0 tăng và biến thiên phức tạp theo góc α do đặc điểm bề mặt cong của cửa bảo vệ. Nghiên cứu khẳng định rằng phần mềm Abaqus là một công cụ hiệu quả trong việc dự đoán và phân tích áp lực nổ tác dụng lên kết cấu cửa công trình, góp phần nâng cao hiệu quả và độ an toàn trong thiết kế, thi công cửa công trình tiếp cận trong thực tiễn. Cùng với đó ảnh hưởng của bán kính cong của bề mặt cong của cửa tới giá trị áp lực sóng phản xạ là phức tạp. Khi tính toán tải trọng tác dụng lên cửa công trình cần chú ý khảo sát giá trị áp lực sóng phản xạ trung bình tại bề mặt cong để có thể tính toán chính xác.

Từ khóa: *Sóng xung kích; áp lực phản xạ; cửa bảo vệ; mô phỏng số; Abaqus; nổ mặt đất; tải trọng nổ; kết cấu hầm.*

Received: 10/10/2025; Revised: 23/12/2025; Accepted for publication: 26/12/2025

❑